

Electronic Supporting Information for:

## **A magnesiothermic reaction process for the scalable production of mesoporous silicon for rechargeable lithium batteries**

An Xing,<sup>a</sup> Jing Zhang,<sup>b</sup> Zhihao Bao,<sup>\*a</sup> Yongfeng Mei,<sup>b</sup> Ari S. Gordin,<sup>c</sup> and Kenneth H. Sandhage<sup>c</sup>

### **Experimental details.**

#### *Preparation of porous Si from SiO*

Mg powder (200 mesh or < 74 μm dia.) and SiO powder (6000 mesh or <2.5 μm dia.) were obtained from, Aladdin Reagent, China and CNPC Powder Material Co., China, respectively. After thorough mixing, the Mg/SiO reactants were heated at 2°C/min in a tube furnace to 300°C for 3 h and then at 2°C/min to 500°C for up to 12 h in a flowing Ar (95 vol%)/H<sub>2</sub> (5 vol%) gas mixture. The powder products were immersed in a 1 M HCl solution for 6 h, followed by immersion in a 5 wt% HF solution for 5 min. The powder products were then washed with distilled water and ethanol, and vacuum-dried at 80°C for 10 h.

#### *Electrochemical tests*

CR2016 cells were assembled to perform electrochemical experiments. The electrodes were composed of 60 wt% of active material, 20 wt% of Super P carbon black, and 20 wt% of sodium alginate as a binder. The electrolyte consisted of a solution of 1M LiPF<sub>6</sub> in a mixture of carbonate-containing vinylene carbonate (Novolyte Technologies, Inc., Suzhou, China). Pure Li foils were used as counter electrodes. The cells were charged and discharged galvanostatically in a fixed voltage window from 5 mV to 1.0 V on a LAND battery test system (Wuhan Kingnuo Electronics Co., Ltd., China) at 25°C. For comparison with the Si produced via magnesiothermic reduction of SiO, Si powder (6000 mesh or <2.5 μm dia.) was obtained from a commercial vendor (CNPC Powder Material Co., China).

#### *Materials characterization*

XRD patterns were obtained at room temperature with a Rigaku D/Max-RB diffractometer using Cu Kα radiation (40 kV, 40 mA). Secondary electron microscopy (SEM) images were obtained with a Philips XL30 FEG field emission scanning electron microscope operating at 10 keV. TEM analyses were conducted with a JEOL JEM-2010 instrument operating at 200 keV. Nitrogen sorption isotherms were collected at 77 K (Micrometrics ASAP 2020 analyzer) after vacuum degassing of the samples at 200°C for 3 h. Values of specific surface area were obtained using the Brunaur-Emmett-Teller (BET) method. The Barrett-Joyner-Halenda (BJH) method was applied to absorption branches of isotherms to obtain pore size distributions.

Supporting Figures

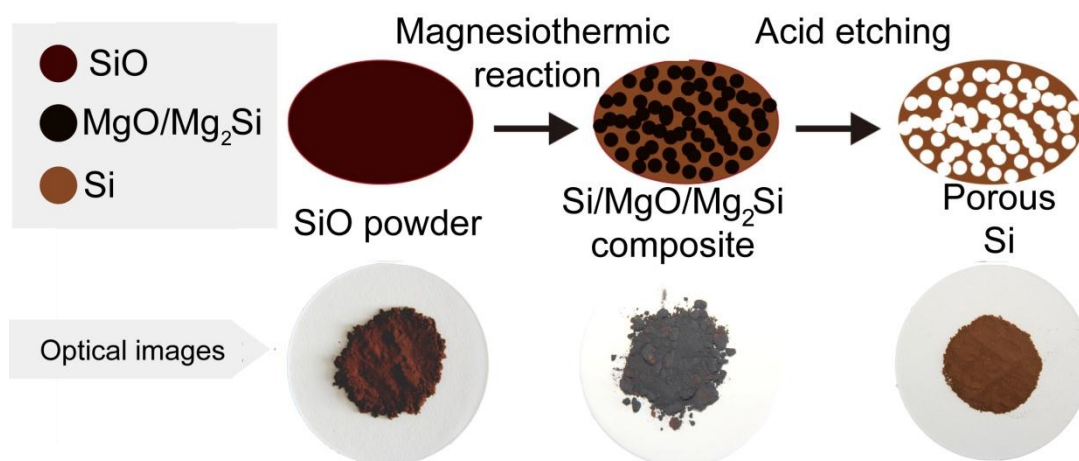


**Figure S1.** Schematic illustration of the formation of porous Si through magnesiothermic reaction of SiO (top row) and associated optical images of materials at each stage (bottom row).

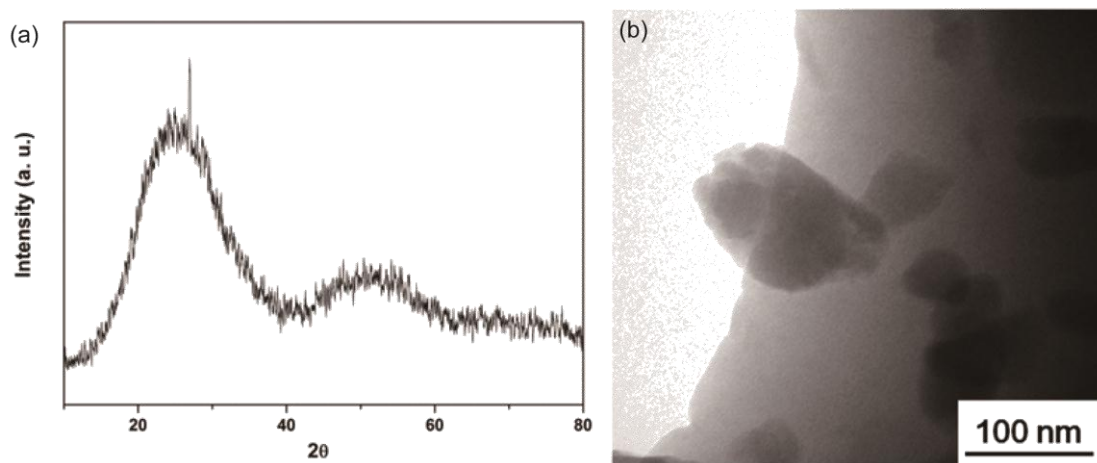


**Figure S2. a**, XRD pattern of SiO powder. **b**, TEM image of starting dense (nonporous) SiO powder.

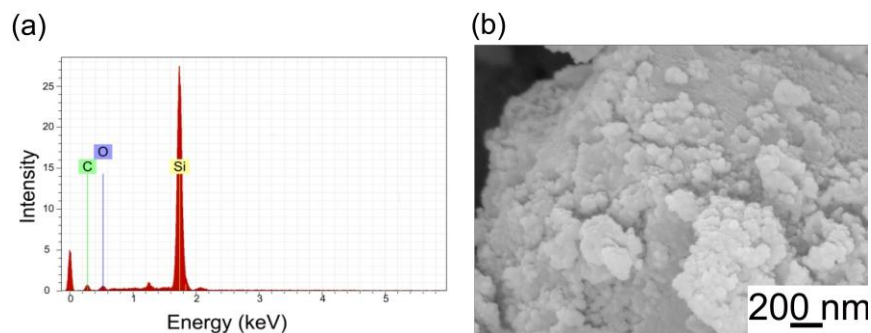


**Figure S3. a and b**, EDX analysis and SEM image of the silicon product prepared via reaction with Mg for 3 h at 300°C and then 12 h at 500°C, followed by acid dissolution of Mg-bearing product phases, respectively.

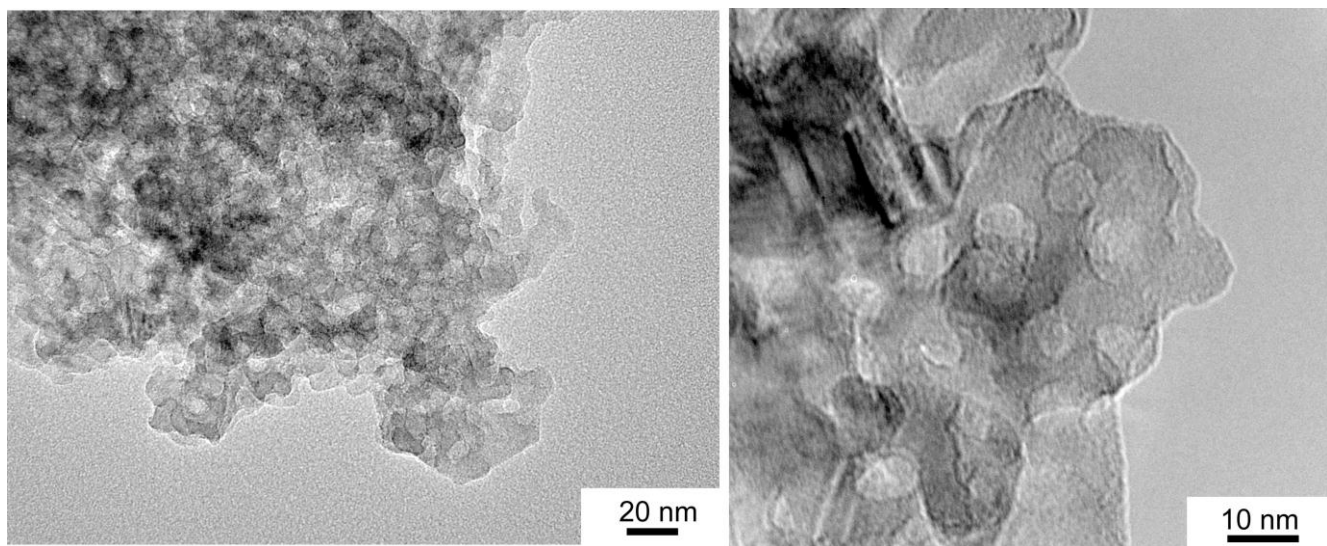


**Figure S4.** High resolution TEM images of silicon product, revealing its porous structure.

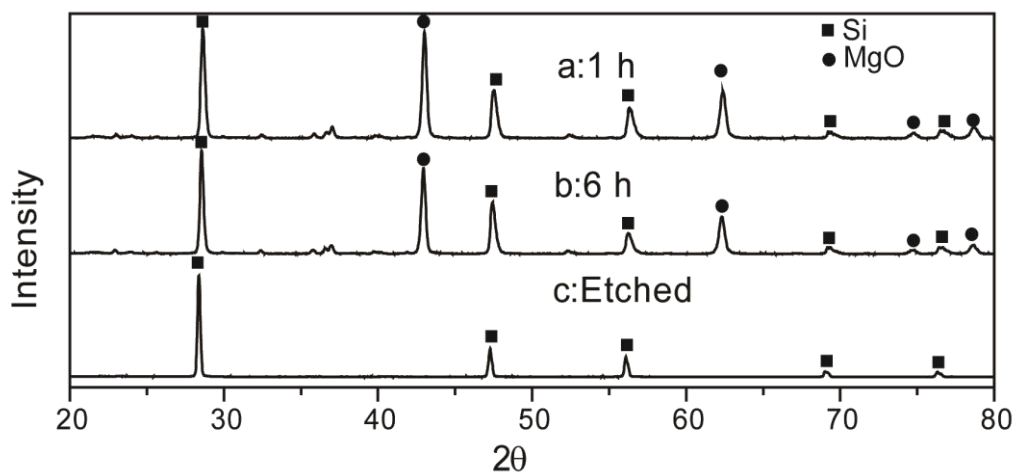


**Figure S5.** XRD patterns obtained from products generated by the reaction of SiO and Mg at 500°C **without the treatment at 300°C**: **a**, for 1 h and **b**, for 6 h. **c**, XRD pattern obtained from the product generated by etching of the sample in **b** with a HCl solution and then a HF solution.

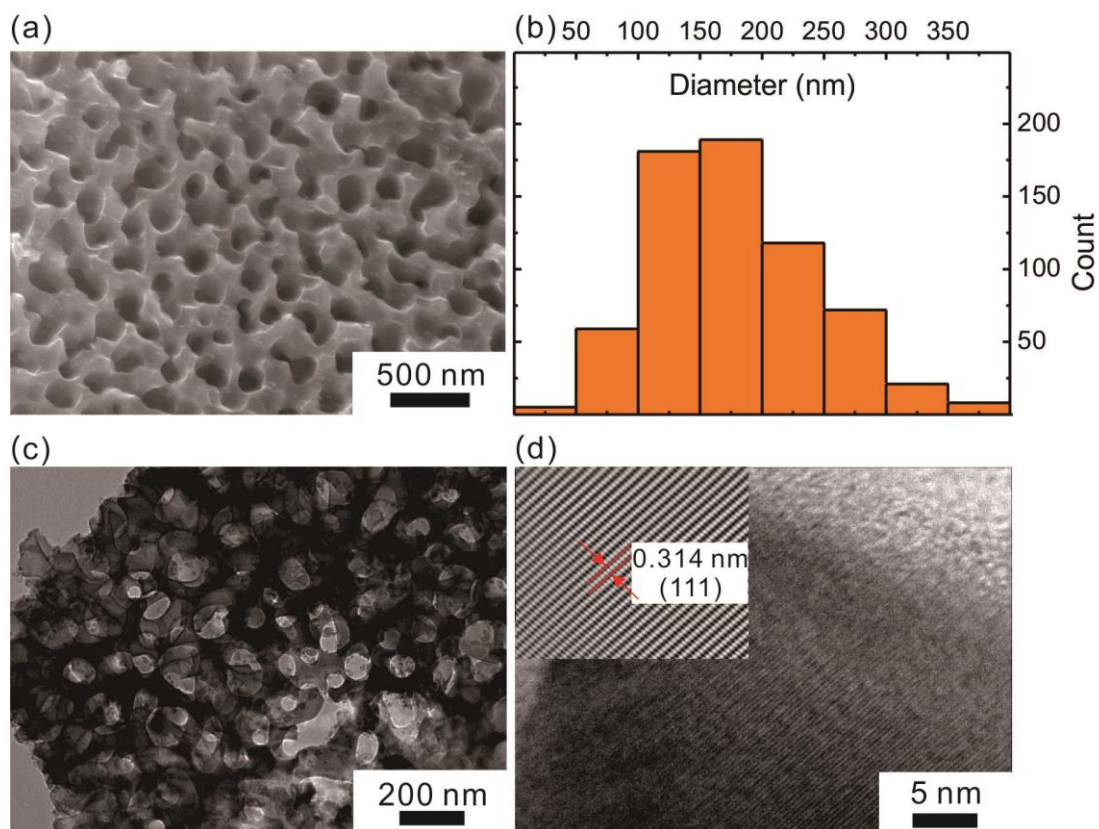


**Figure S6.** Characterization of the product **without the treatment at 300 °C**: **a**, SEM image of the product at high magnification. **b**, Pore size distribution obtained from SEM images of the product. **c**, **d**, Low and high magnification bright field TEM images of the silicon, respectively (the inset in **d** reveals part of the image in **d** after Fourier filtering)

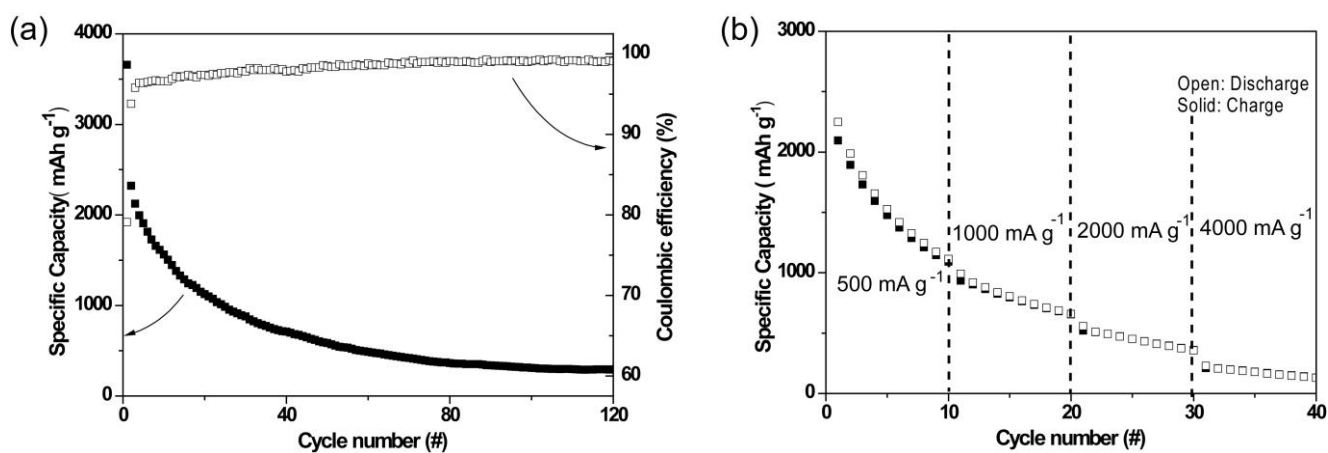


**Figure S7. a, b**, Cycling performance and rate performance of the product **without the treatment at 300 °C**, respectively.

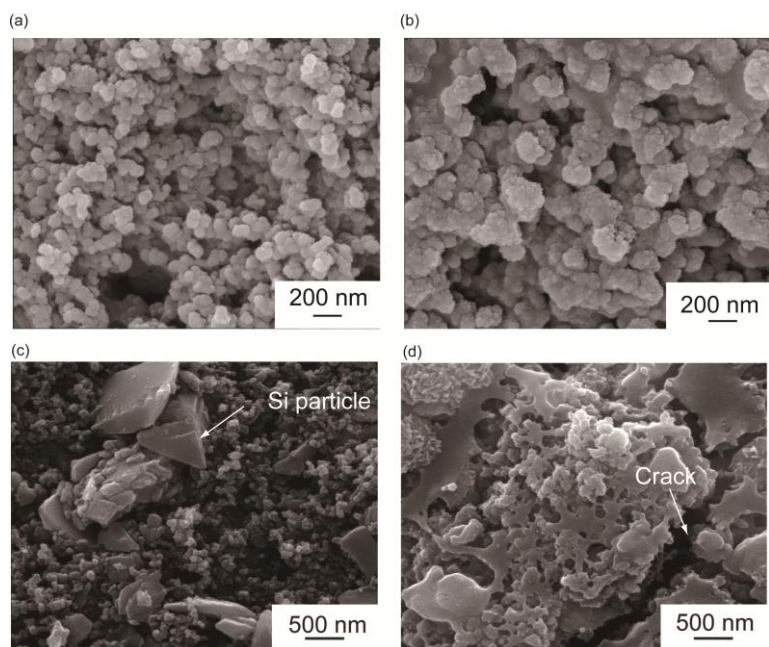


**Figure S8.** SEM images of porous nanocrystalline silicon-based electrodes **a**, before the cycling and **b**, after the cycling. SEM images of solid silicon-based electrodes **c**, before the cycling and **d**, after the cycling.